HIGH SCHOOL EDITION
Journal of Student Research
Volume 11 Issue 4 (2022)

Design of a Novel Kresling Origami Lumbar Disc Replacement for Degenerative Disc Disease

Xinyi Zhang[1], Jessica Zheng[1], Mulan Jiang[#] and Zimi Zhang[#]

[1] South Brunswick High School, Monmouth Junction, NJ, USA
[#]Advisor

ABSTRACT

Though it is normal for spinal discs to show signs of wear and deterioration with age, this process may result in degenerative disc disease (DDD), causing pain, stiffness, and even physical deformity. DDD affects 40% of people aged 40 years old and increases to 80% for those aged 80 years or older. Lumbar disc replacements (LDRs) are commonly used as a surgical intervention for DDD. Unfortunately, currently marketed LDRs present a myriad of problems that lead to a clinical failure rate of up to 26% at a two-year follow-up report. Patients with underlying conditions such as diabetes experience even higher rates of clinical failure. Root causes for complications include incorrect sizing of the implant, lack of mobility, and material choices that do not allow for proper integration into the body. Our project proposes a novel design that will replicate the properties of natural lumbar discs and mitigate these complications. This design consists of porous titanium (Ti-6AL-4V)/chitosan sponge composite endplates that can be loaded with compounds to prevent infection and accelerate fusion with the vertebrae surrounding the LDR. A polyurethane Kresling Origami-inspired insert will be sandwiched in between the endplates, allowing the LDR to adjust its size for optimal fitting and provide shock absorption, stability, and mobility to the spinal column. Methods for executing this design are also proposed, along with mechanical and biological tests to be conducted. This paper is the first part in a series of studies that will culminate in assembling and testing the final LDR.

Introduction

Degenerative Disc Disease (DDD) is one of the most frequent causes of back pain and broadly refers to the gradual wearing down of a spinal disc (Figure 1). Generally, disc degeneration is a natural course of aging but varies greatly in its severity, especially with increasing age. DDD affects 40% of people aged 40 years old and increases to 80% for those aged 80 years or older (Medical Advisory Secretariat, 2006). Common symptoms include lower back pain, pain near the site of the degenerated disc, loss of mobility, and muscle tension. More severe effects of DDD often turn the dulling pain into shart, stabbing spikes of pain. Those suffering from DDD have difficulty expressing physical motions that require increased spinal and lower body mobility, such as bending, lifting, twisting, and even standing. Nonsurgical treatments can be used to relieve pain, but it is estimated that up to 30% of people with DDD will be unresponsive and required to seek surgical treatment (Medical Advisory Secretariat, 2006).

A common intervention for DDD is lumbar disc replacement (LDR), which is a surgical procedure that involves replacing a degenerated disk with an artificial disc created to mimic the disc's natural movement; as a result, there is a great clinical need for effective LDRs. A spinal disc facilitates four motions: bending backwards/forwards, bending sideways, twisting rotationally, and standing. Each action exerts different forces upon the spinal disc as demonstrated in Figure 2. A lumbar artificial disc ultimately seeks to reduce the instability and minimize the muscle tension caused by the small motions at the disc-level. Despite the large clinical

demand to treat lumbar degenerative disc disease, widespread adoption for LDR solutions has not occurred due to the recurring pattern of complications found in patients who have undergone the solutions.

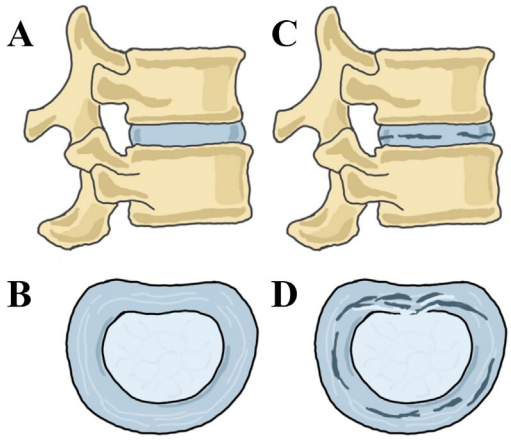

Figure 1. Anatomy of a healthy vs. degenerated spinal disc. A) Lateral view of a healthy spinal disc. B) Superior view of a healthy spinal disc. C) Lateral view of a degenerated spinal disc. D) Superior view of a degenerated spinal disc.

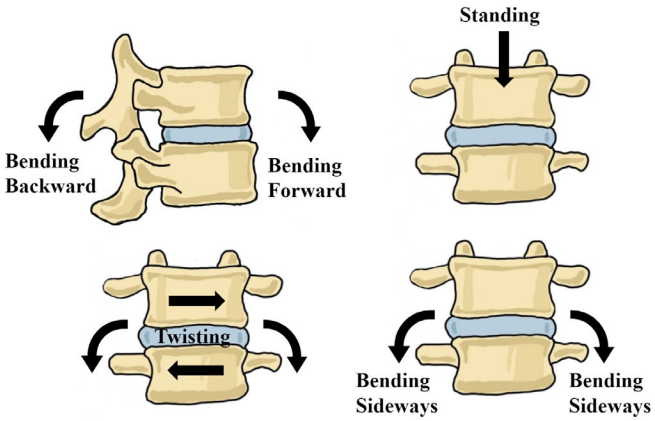

Figure 2. Motions that lumbar spinal discs facilitate. These motion requirements were all considered during the design of the proposed LDR.

Unfortunately, currently marketed LDRs present a myriad of problems that have a clinical failure rate of up to 26% at a two-year follow-up report (Pettine, 2017). The primary complication of LDR is incorrect sizing, leading to dislocation, dislodging, loosening, narrowing of the spine (stenosis), increased pain, fractures, and loss of motion. (Johns Hopkins, 2022), Furthermore, there are substantiated concerns over the design and the material used for disc replacements. Non-porous titanium endplates, currently used in marketed devices, give minimal opportunity for the vertebrae and the endplates to fuse, a crucial factor in determining the success of the implant. The non-porous titanium alloy, Ti-6AL-4V, is used in many medical implants, but has a Young's Modulus (YM) of around 110 GPa, which is much higher than that of bone (10-30 GPa) (Niinomi & Nakai). YM is the measure of elasticity or stiffness of a material when force is applied. This drastic difference in GPa leads to a lack of shock absorption and runs the risk of stress shielding, which may lead to implant loosening and bone atrophy, a reduction in bone density due to the excessively fast breakdown of the bone substance and structure (Sigma Aldrich, 2022).

Currently, a clinical alternative to LDR is fusion spine surgeries, a procedure that uses bone to connect two vertebrae that are next to each other. (Spine Universe, 2021) Despite the rising rates of fusion surgeries in particular, these procedures have several potential issues, such as loss of mobility, failure to achieve a solid fusion mass (pseudarthrosis), adjacent segment degeneration (ASD), etc. Additionally, some patients may have other health concerns that prevent current LDR methods from working effectively. Diabetic patients tend to have lower vitamin D levels, resulting in minimal osseointegration from poor bone strength, density, and overall quality (DeJesus, 2020). Compared to non-diabetic patients, fractures, corrective surgeries, and further disc damage are elevated risk factors for those undergoing LDR surgery. Diabetes also increases susceptibility to spinal infections from surgeries, which may result in vertebral osteomyelitis, lumbar spinal stenosis, or other spinal infections (Hillson, 2018). While the proposed solution can suit the needs of the general population suffering from DDD, it has great potential to mitigate common risk factors of current LDRs for patients suffering from other health concerns, like diabetes.

Current Approaches

The first LDR was the Charité in 2004, which was removed from the market in 2012 due to Charité Disc Complications, including blood transfusion, death, paralysis, increased back/spinal pain, cracked vertebrae, additional stress and adjacent disc damage, spinal fractures, nerve damage, vein and/or artery trauma, etc. The second was the ProDisc-L in 2006 which remains a medical device, but it is not commonly used due to frequent dislodging, increased tendency to wear, heightened risk of corrective surgery, and a lack of mobility from its ball-and-socket structure (Yue et al, 2016).

The first modern LDR was the ActivL Artificial Disc. Inserted into the spine, the activL disc are only available in four sizes (26×31, 28×34.5, 30×39, and 33×40 mm) (anteroposterior × lateral dimensions), meaning their product is not customized to the specific height needed to fit between the patient's spine discs and runs the risk of incorrect sizing. ActivL notes that not all of the patients will achieve motion after treatment, and they will only achieve four degrees of freedom with a lack of side-to-side movement (Yue et al, 2016). The overall successful integration rate of the ActivL disc with range-of-motion is 50% (FDA).

Both the ActivL and ProDisc-L are the two primary LDRs available on the market and still hold FDA approval, but each suffer their own set of problems. Along with the complications previously mentioned, both are made from cobalt-chromium with a YM of ~220 GPa in comparison to bone (10-30 GPa). Most critically, both have limited size options available that leave a vast majority of the patients forced to undergo surgery with an ill-fitting artificial disc that may lead to even greater problems post-surgery. The two primary sets of complications, 1) incorrect sizing and 2) material/design complications, make successful, widespread adoption of the two currently-available LDRs for patients difficult given the scope of the problem.

Another common LDR engineering approach is a general ball-and-socket implant (Figure 3). However, this leads to a large amount of wear due to the curved surface of the ball, which can lead the ball to fall out of the socket. Replacing or recovering the ball requires a much lengthier and more invasive surgery process. The ball-and-socket model also does not provide any shock absorbance or a similar YM to bone.

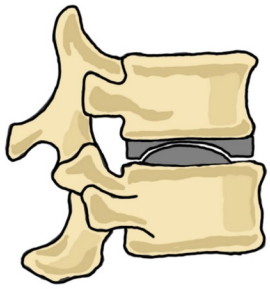

Figure 3. Ball-and-socket LDR.

The idea of using origami in lumbar disk replacements was previously explored by Brigham Young University's research. (Editors, 2016). However, there has not been further development in this area. Nonetheless, the proposed design incorporates elements that have been promising in previous research, such as the use of a bioactive coating and porous titanium. Furthermore, the bioactive coating's antibacterial properties may become a safer, more reasonable option for patients suffering from other underlying health conditions, such as diabetes. The proposed kresling origami pattern with flat-fold properties also offers a customizable LDR which eliminates the most common problem of ill-fitting disc replacements in current approaches.

LDR Design

To combat the issues listed previously, we are proposing a new design for an artificial LDR (Figure 4). From bottom to top, the porous titanium endplates (a) serve to match the natural bone and allow the bone to form a 3D interlocking bond with the implant. Titanium will be used as the endplate material because of its strength, biocompatibility, and proven record of success as an implant material.

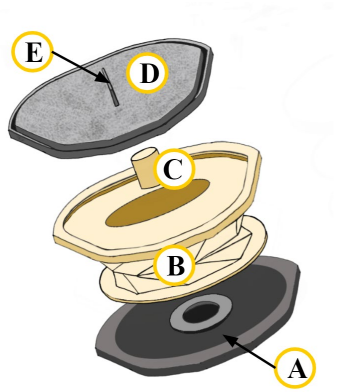

Figure 4. Proposed solution design viewed from bottom to top. A) Top endplate with the polyurethane spring core holder (shown)and porous titanium/chitosan composite (not shown.) B) Kresling origami insert, with a structure on the end closer to the bottom that allows for wrapping around the bottom endplate (mechanical adhesion.) C) Polyurethane spring core. D) Bottom endplate with the polyurethane spring core holder (not shown) and porous titanium/chitosan composite (shown.) E. Keel (found on both endplates.)

The endplates will surround an interior Kresling Origami insert (b) that will consist of two stacked Kresling Origami structures in opposite directions (Figure 5). The bottom part of insert will be capped off with a structure that will allow the insert to mechanically "lock" into the bottom endplate, which will be referred to as "mechanical adhesion." The top end of the insert would remain detached from the endplate, but will be closed off. This way, the insert will be free to twist against the endplate. This insert will lend the implant in higher compressibility, shock-absorption, and greater stability than currently available options (Kidambi & Wang, 2020). Most importantly, this origami design will allow for the implant to flatten and expand so it can adjust to the varying spaces and angles between vertebrae in different bodies, reducing the risk of improper fitting.

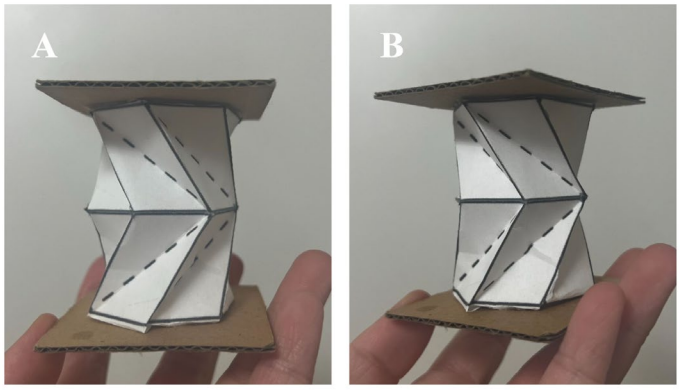

Figure 5. Double stacked, opposite twisting Kresling structure. A) Front view. B) Side view.

A polyurethane spring core (c) will serve to prevent implant flattening and add to shock absorption capabilities. Porous titanium endplates will be filled with a chitosan sponge (d). Chitosan has excellent biocompatibility, biodegradability, and antimicrobial properties (Polo-Corrales et al., 2014). Furthermore, chitosan sponges improve cell attachment and proliferation in titanium parts (Guo & Li, 2015). If loaded, the porous Ti-chitosan sponge composite allows for the sustained release of antibiotics such as vancomycin and growth factors such as bone morphogenetic protein-2 (BMP-2) to prevent infection and promote bone fusion with vertebrae (Pawar et al., 2019). The porosity and the bioactive endplate coating will increase the speed of fusion between the artificial disc and vertebrae, reducing the risk of implant dislodging. Finally, the keel (e) will hold the implant firmly in place to prevent unnatural movement.

Endplates

The top LDR endplate footprint (Figure 6) will be 39mm x 30mm in accordance with the dimensions of LDRs currently on the market. The bottom LDR footprint will be 38mm x 29mm to account for the thickness of the origami insert that will fit around it. To minimize the height the endplates would take up but also ensure that the endplate would be strong enough to withstand the normal load and forces endured by a natural lumbar disc, a height of 2.0 mm was chosen for the endplate.

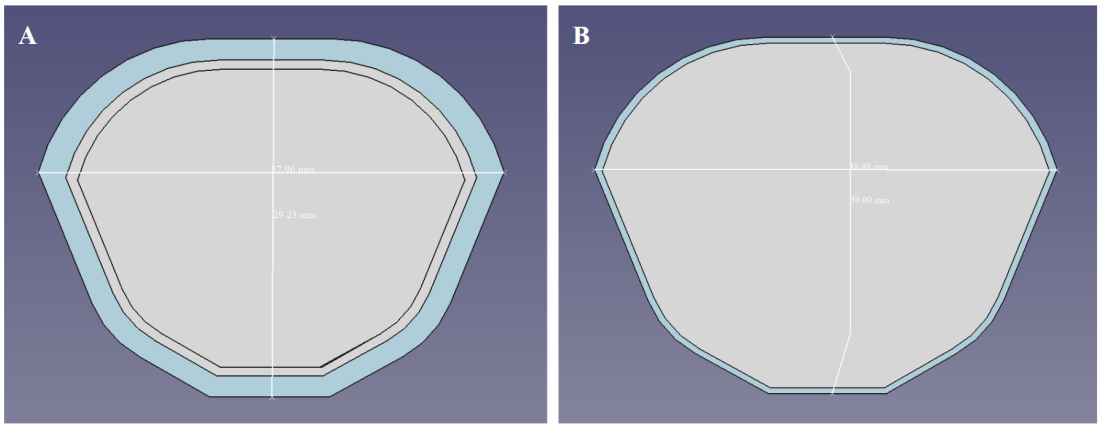

Figure 6. Titanium endplate footprints modeled on FreeCAD. The bottom endplate footprint (A) is 38mm x 29mm. The top endplate footprint (B) is 39mm x 30mm.

Three iterations of the titanium endplate were tested to determine the optimal mechanical adhesion design that the origami insert will fit around (Figure 7): one with a "locking" mechanical adhesion mechanism (7A), one with a "wrapping" mechanical adhesion mechanism (7B), and one with no mechanical adhesion mechanism, which would serve as the top endplate (7C). A small indent was cut on the underside of the top endplate to ensure the insert stays capped in even with no mechanical adhesion mechanism (7D). All endplates had a circular holder on the underside to hold the spring core (7D).

The porous titanium endplates were first 3D modeled in FreeCAD in a completely solid form consisting of two parts. One part would remain solid throughout its composition and the other would be made into a porous structure. The three models were then printed as test samples with plastic filament. After examining how the models would allow for mechanical adhesion to the insert, it was determined that the mechanism in version A was not feasible given the size of the implant, so we proceeded with versions B and C only, with version B serving as the bottom endplate and C serving as the top endplate.

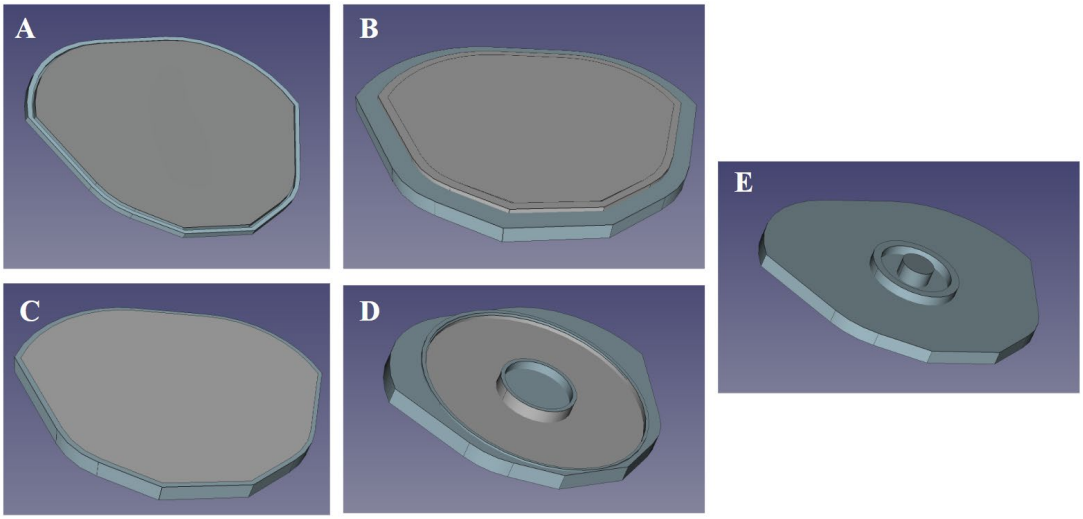

Figure 7. Three endplate versions modeled on FreeCAD (A, B, C), top endplate groove to hold origami insert in place (D), and the holder for the polyurethane core with a protrusion to keep the core in place (E). The gray portions represent porous titanium portions which would be created in nTopology in a later step. Keels were omitted for efficient printing and testing.

Using the finalized CAD models and nTopology software, adjusting the porosity of the endplates would give them a YM close to natural bone in order to prevent stress shielding. It has been shown that 30% porosity titanium has a YM that matches that of human cortical bone (Oh et al., 2002). This porosity was achieved after the models were uploaded in the nTopology software and intersected with a 1.5 mm cell size Schwartz lattice body (Figure 15). Through the functions available on nTopology, the volume of the porous version of the top endplate was determined to be 1,311.8934 mm^3 whereas the volume of the solid version of the top endplate was 1,875.7046 mm^3. These numbers were plugged into Equation 1 to yield a porosity of 30.058635%.

Equation 1: Porosity Equation (%)

$$Porosity\ (\%) = \frac{(Volume\ of\ Solid\ Structure\ -\ Volume\ of\ Porous\ Structure)}{Volume\ of\ Solid\ Structure} \times 100\%$$

Kresling Origami Insert

Origami-inspired structures have combined the sciences of topology and geometry to provide unique structures with a rich design space. The ability to fold various structures mathematically allows for new opportunities to utilize its properties in creating new innovations for healthcare and medical purposes. More specifically, Kresling origami is a newly-studied pattern of origami that offers great potential in bioengineering medical devices due to its flexibility, range-of-motion, multi-stability, and the diversity of structures available. The Kresling pattern also falls into the category of flat-fold origami. Flat-fold origami has the ability to maintain its original structure, without creating new folds, when pressure is exerted on it until the structure becomes flat (Figure 8). When placing it between two spinal discs, it would expand, exiting its "flat-form" to mitigate any complications that would arise from incorrect sizing. Though the fully expended model would not be used, the compressibility and extra "room" is used to provide shock absorption.

The traditional pattern for the Kresling origami structure has ten self-organized folding patterns, formed by inclined and elongated parallelograms (mountain folds; solid lines), divided by a valley fold (dotted line). This self-organized pattern comes naturally from the twist buckling of a cylinder. While the ten-fold pattern is traditionally used for larger structures, human spinal discs and currently marketed and FDA-approved discs are much smaller. Thus, further research was conducted on smaller Kresling prototypes, including a 4, 5, 6, 7, and 8-fold structure. These prototypes all consisted of two stacked Kresling structures with opposite directions of folding. This structure serves to prevent the implant from twisting in one direction as it flattened and also added to the structure's stability. Being able to determine the optimal number of folds according to which prototype excels in the areas of spinal movement needed for successful integration will provide more insight into which pattern to use for how the finalized, manufactured biomedical device is proposed.

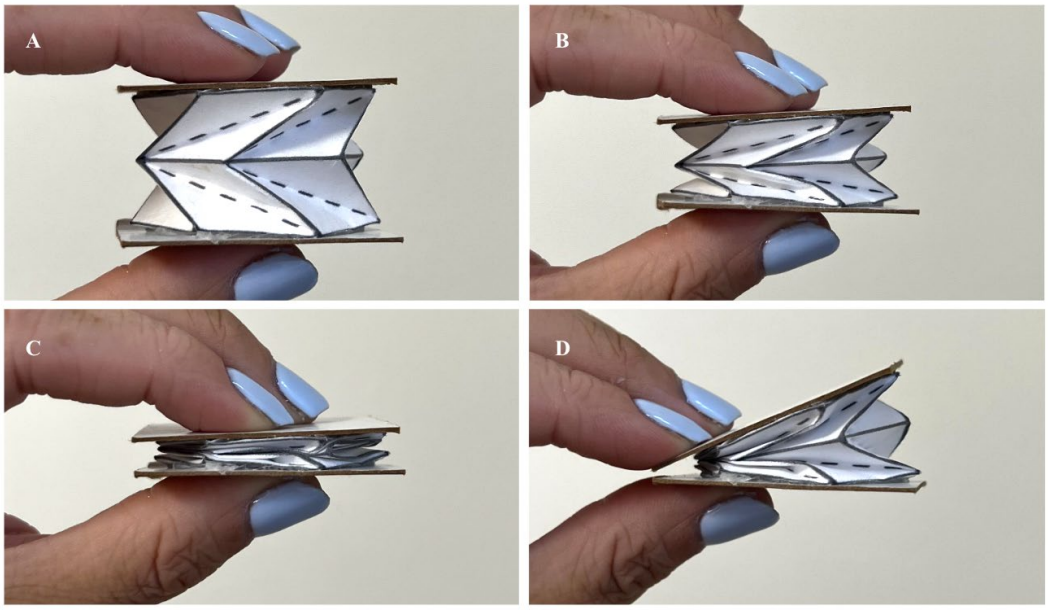

Figure 8. Pressure applications of Kresling origami structure. A) Fully expanded. B) Partially compressed. C) Fully compressed. D) One-sided pressure.

Furthermore, a customizable polyurethane spring core will be attached in the center to establish the minimum height of the disc while providing more elasticity and shock absorption. This structure will allow many degrees of freedom in motion while reducing risk of wear that is present in ball-and-socket designs.

Origami Pattern Evaluation

Research was conducted on the optimal, feasible amount of "Kresling" folds (4, 5, 6, 7, or 8 folds) (Figure 9) evaluated on three properties 1) Recoil percentage 2) spinal twisting and 3) qualitative observations.

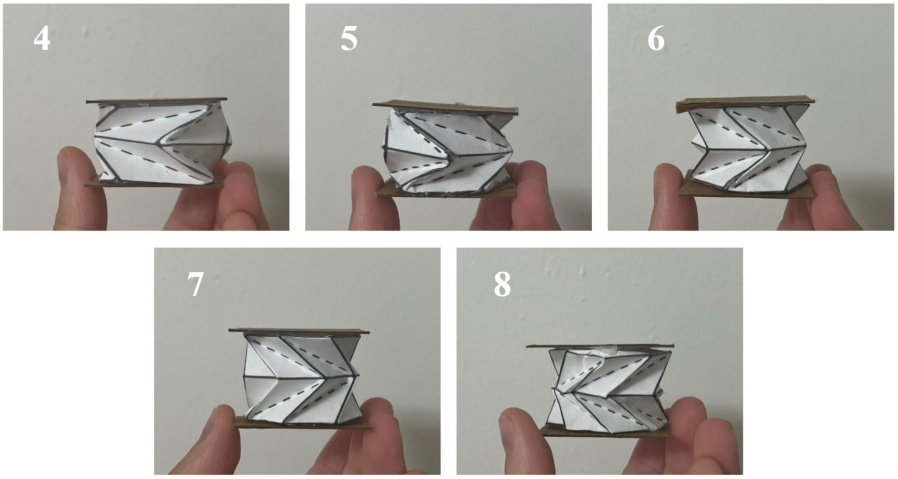

Figure 9. Various Kresling fold structures that differ by number of Kresling folds/units. Each number corresponds to the number of Kresling folds/units.

1. Recoil: To determine which of the structures had the most recoil, mimicking the flat-fold properties when surgically inserted, the average percent recoil of the various origami folding versions was determined by measuring the mm of immediate "recoil" when pressure is applied directly to the structure.
2. Spinal Twisting: When twisting our doubled Kresling origami structure, the "twist" of the spinal disc is maxed out when half the structure enters its flat-fold state (Figure 10).
3. Qualitative Observations: To select the most sufficient Kresling origami version, each prototype's qualities were observed and supported using recorded standard quantitative data.

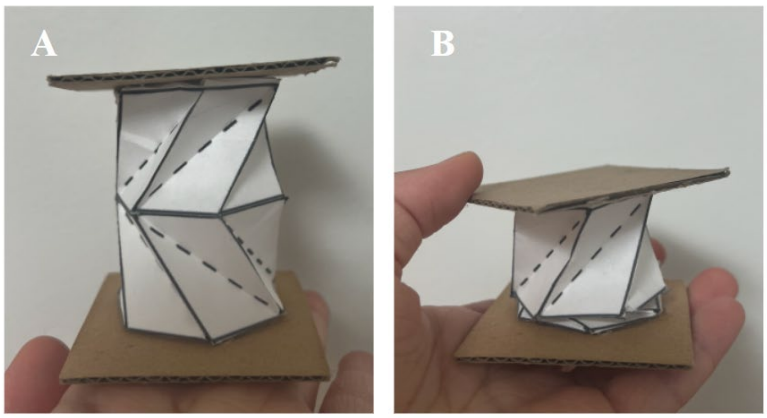

Figure 10. Maximum twist of Kresling structure. A) No movement. B) Max spinal twist. Images were taken from a prototype that was scaled up in height.

Origami Pattern Evaluation Results

The tables below depict the data collected from 5 Kresling origami structures with different numbers of "Kresling folds" (4, 5, 6, 7, or 8) made out of traditional paper.

Table 1. Origami Folding Recoil Percentage (%) vs number of Kresling folds trials.

Recoil (%)					
Trial #	**4 Folds**	**5 Folds**	**6 Folds**	**7 Folds**	**8 Folds**
1	66.7	75.0	91.3	75.0	72.0
2	66.7	72.7	91.3	72.9	72.0
3	66.7	77.3	90.2	75.0	73.0
4	67.9	76.1	90.2	75.0	71.0
5	66.7	75.0	91.3	73.9	72.0
AVG	**66.9**	**75.2**	**90.9**	**74.4**	**72.0**
STDEV	**± 0.0055**	**± 0.0168**	**± 0.0059**	**± 0.0093**	**± 0.0071**

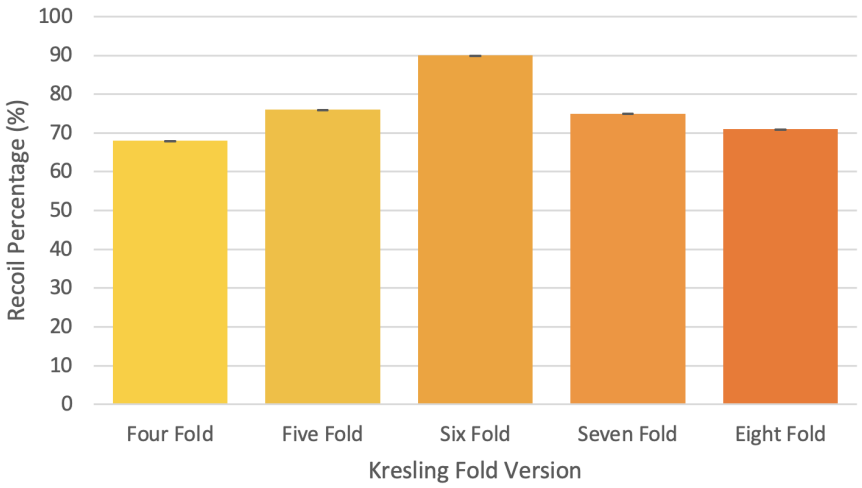

Figure 11. Graph of average origami recoil percentage (%) vs number of Kresling folds.

Table 2. Origami spinal twisting amount (°) vs number of Kresling folds trials.

Spinal Twisting (°)					
Trial #	**4 Folds**	**5 Folds**	**6 Folds**	**7 Folds**	**8 Folds**
1	18.0	15.0	20.0	18.0	15.0
2	18.0	14.0	19.5	19.0	16.0
3	16.5	15.5	20.0	18.0	15.5
4	16.8	15.0	20.0	18.3	15.0
5	17.0	15.0	19.5	18.0	15.0
AVG	**17.3**	**14.9**	**19.8**	**18.3**	**15.3**
STDEV	**± 0.707**	**± 0.548**	**± 0.274**	**±0.433**	**± 0.447**

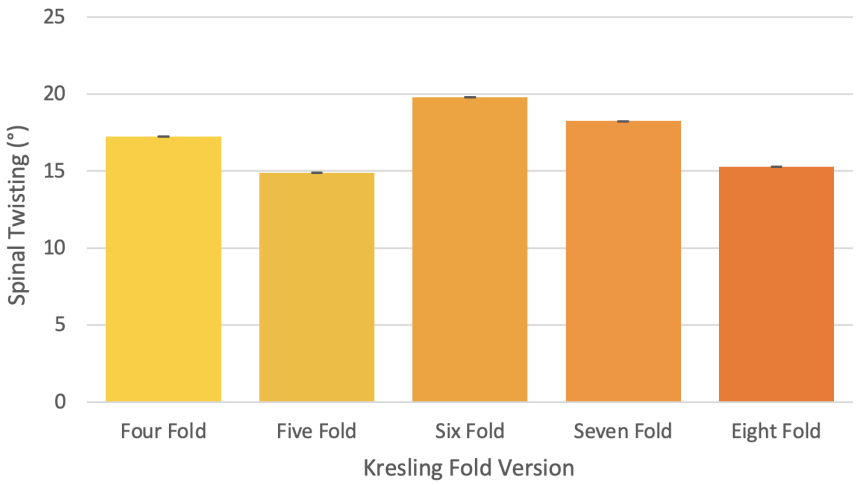

Figure 12. Graph of average origami spinal twisting amount (°) vs number of Kresling folds.

Table 3. Dimensions and relative properties vs number of Kresling folds.

Dimensions and Relative Properties						
Folds	**Max Height (mm)**	**Min Height (mm)**	**Max Angle (°)**	**Dimensions (mmxmm)**	**Max H to W Ratio (mm:mm)**	**Min H to Max H Ratio (mm:mm)**
4	21	4.5	20	34x24	0.875	0.214
5	22	4.25	20	35x32	0.688	0.193
6	23	4	20	36x27	0.852	0.174
7	24	3.5	20	32x30	0.800	0.146
8	25	3.5	20	33x25.5	0.980	0.140

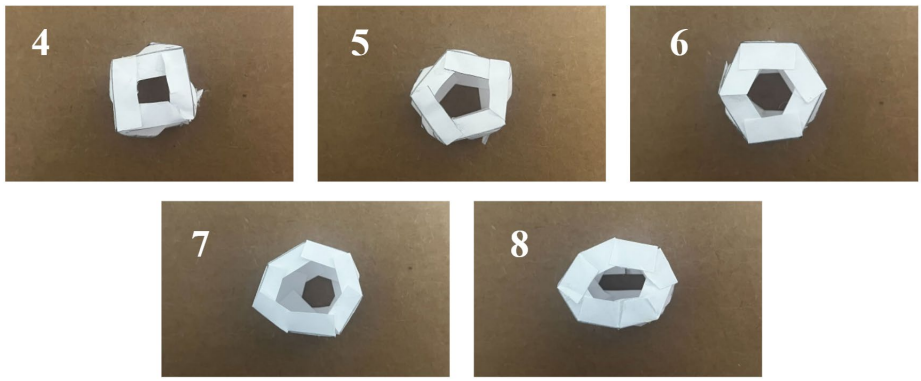

Figure 13. Bird's eye view of Kresling fold structures. Each number corresponds to the number of Kresling folds.

As evidenced in the collected data, the structure with 6 Kresling fold demonstrated superior results in all three of the characteristics that were evaluated. Thus, the 6-fold Kresling origami pattern shown in Figure 14 was the one selected for the final LDR design.

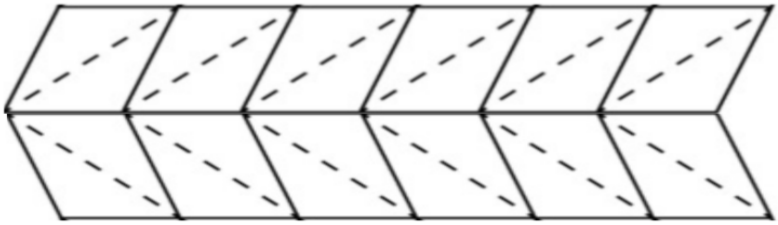

Figure 14. Folding pattern proposed for the Kresling origami insert portion of the LDR design. Image is scaled up. Real dimensions are (11.5 cm x 3.2 cm).

Expected Physical Specifications of the LDR

The LDR endplate will be 39mm x 30mm and the LDR will have a height ranging from 8 mm to 23 mm (from flattened to fully expanded). It is important to note that the fully expanded state will almost never be utilized. 23 mm merely serves as the upper limit to what sizes our LDR can accommodate. For reference, the lowest available height on the market currently is the ActivL disc, which has a height of 8.5 mm, whereas the average natural lumbar disc height falls between 7 and 10 mm tall (Okpe, 2021). In the end, our design will provide a more natural and better healing solution for DDD surgical interventions.

Proposed Materials and Methods

Endplates

Using the available resources and funding available, the following steps have been carried out: As stated in the Design section, the porous titanium endplates were first 3D modeled in CAD software. Final models were uploaded in the nTopology platform and intersected with a Schwartz lattice body with 1.5 mm cell size to create the porous structure (Figure 15). A sample piece for future testing was also modeled and printed using the same process. The endplates and sample piece were 3D printed in Ti-6AL-4V using the Sculpteo service, as shown in Figure 16.

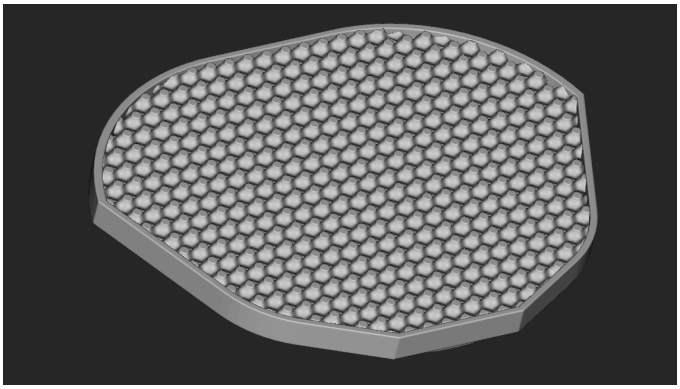

Figure 15. Porous titanium endplate C modeled on nTopology.

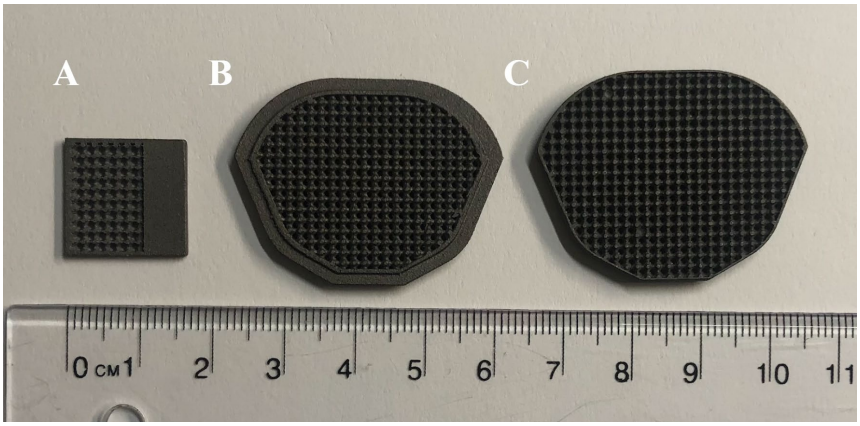

Figure 16. 3D printed porous titanium endplates. A) Sample piece. B) Bottom endplate. C) Top endplate.

Kresling Origami Insert

Three methods to create the Kresling origami insert were considered: 1) 3D printing 2) molding 3) folding. While 3D printing the insert in its final form would have allowed for greater reproducibility and minimal error in creating the structure, the Kresling structure proved to be difficult to model on currently-available software and complicated to print given the small size and thickness of our insert. However, given the small size of the insert, using the molding method gives way for human error and exacerbated material flaws that weakened the final insert's structure. For our rough prototype, the folding approach was used, in which the final origami pattern (Figure 14) was printed onto paper and affixed to a clear polyester sheet. Then, the polyester sheet was folded according to the pattern to create the final Kresling origami structure. The structures that would allow the insert to mechanically "capture" the endplate were also made with polyester and then attached to the Kresling origami using Permabond 731, an adhesive which passes standards for biocompatibility cytotoxicity testing.

It was ultimately decided that the best approach for the final prototype would be a combination of 3D printing and folding, wherein the flat origami pattern with grooves, as shown in Figure 17A, would be 3D printed in elastomeric polyurethane, folded, and then glued together using Permabond 731. The part of the insert that would allow for mechanical adhesion of the origami structure to the endplates (Figure 17B) and the polyurethane spring core (Figure 17C) would be 3D printed directly in elastomeric polyurethane and attached to the Kresling origami structure using Permabond 731.

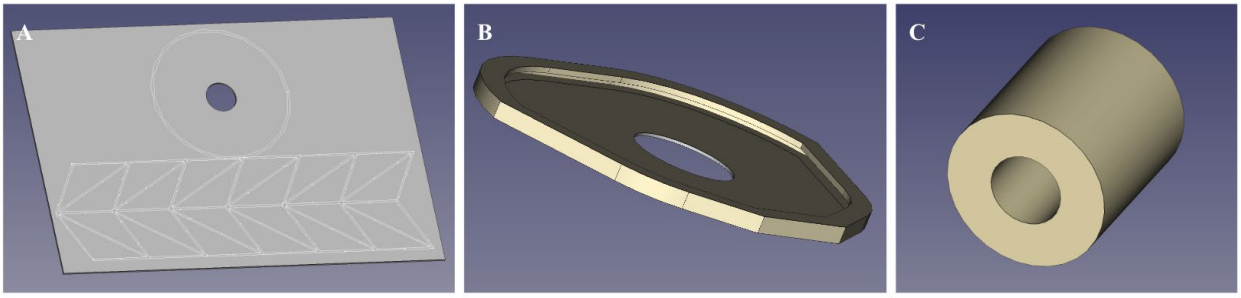

Figure 17. CAD models for assembling the Kresling origami insert. A) Flat origami pattern. B) Structure that would allow for mechanical adhesion to the bottom endplate. C) Polyurethane spring core.

Porous Ti-6AL-4V/Chitosan Sponge

The porous Ti-6AL-4V/chitosan sponge composite will be made by the procedure described by Guo & Li, 2015. 85% deacetylated chitosan will be dissolved in .2 M acetic acid and the solution will be gently stirred for 2 h at 50°C. The resulting 1 wt% concentration chitosan solution will then be neutralized to pH 7.4 using 1 M NaOH. The porous Ti-6AL-4V endplates will be placed in a petri dish and chitosan solution will be casted into each part. Parts will be frozen at −20 °C for 12 h and then left to freeze dry overnight at a freeze-drying temperature of −80 °C (Guo & Li, 2015). The porous Ti-6AL-4V/chitosan sponge composite will then be loaded with vancomycin solution and dried with a hot air oven at 40°C for 2h (Pawar et al., 2015). Alternatively, the sponge can be loaded with a growth factor such as bone morphogenetic protein-2 (BMP-2).

Scanning Electron Microscopy (SEM)

Analyzing the endplates under a Scanning Electron Microscope will offer data pertaining to the endplate's topography and composition. This study is especially critical to the success of our implant because it will provide increased detail of the pores in the titanium, as well as their capacity to hold antimicrobial properties and promote osseointegration after biological testing. Furthermore, the effects of the various mechanical testing may be observed in greater detail through SEM imaging.

Mechanical Testing

The following mechanical tests should be conducted on the final prototype: cyclic load, shear, wear, and compressive strength testing. Using a cyclic load test machine will provide data on how many "cycles" of the implant are effective until the structure begins to fatigue. Testing both shear and wear will allow us to determine the theoretical life-span of the final implant, as well as any potentially weak areas on our implant that may need to be strengthened. A compressive strength test will be conducted to measure the maximum amount of compressive load the implant can bear before fracturing which may aid us in altering the design or material choice of the current final implant.

Biological Testing

After the mechanical testing, two biological tests will be conducted, an MTT cell viability assay and an antibacterial assay. The MTT cell viability assay in combination with a bone tissue culture will be used to quantify the amount of cell growth and viability on our endplate to test its potential for osseointegration (Fu et al, 2017). This should be tested whether or not the BMP-2 is loaded into the composite. If the vancomycin is loaded into the composite, the antibacterial assay will screen its antimicrobial and drug release properties.

Assembly

The final prototype can be assembled with the polyurethane spring core fitting into its holder on the bottom endplate and the bottom part of the insert wrapping around the bottom endplate so that they are mechanically adhered (Figure 18). The top part of the insert will fit into a groove on the underside of the top endplate, thus enabling the LDR to allow for twisting motions inside the body.

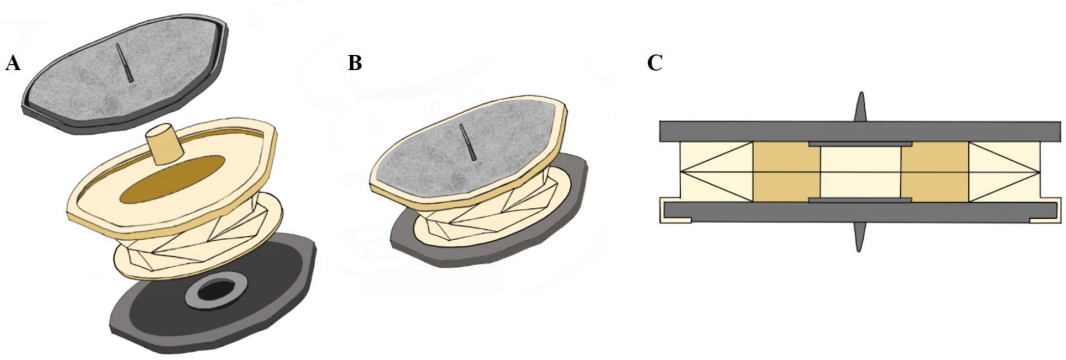

Figure 18. Assembly plans and structural details for the LDR. A) Parts of the LDR, bottom to top. B) Fully assembled LDR (bottom endplate up). C) Cross section of the LDR (bottom endplate down.)

Rough LDR Prototype

A rough prototype, using the parts described in the Endplates and Kresling Origami Insert parts in the Proposed Materials and Methods section, was assembled. The rough prototype, while possessing some distinctions from our expected final prototype, was important for us to get a general idea of the physical and functional specifications of the design, as shown in Table 4 and Table 5, respectively.

Table 4. Physical specifications of rough LDR prototype.

Physical Specifications	
Weight (g)	14.157
Endplate footprint (mmxmm)	39x30
Endplate height (mm)	2.5
Fully Expanded Height of LDR (mm)	22.1
Fully Compressed Height of LDR (mm)	8.2
Max H to W Ratio (mm:mm)	0.631

Table 5. Functional Specifications of Rough Prototype.

Functional Specifications		
Trial #	**Recoil (%)**	**Spinal Twisting (°)**
1	97.2%	2.1
2	99.9%	1.8
3	98.6%	2.3
4	97.3%	1.7
5	99.1%	1.7
AVG	**98.4%**	**1.9**
STDEV	**± 0.0116**	**± 0.268**

Discussion

Origami Pattern Evaluation

The section titled "Origami Pattern Evaluation Results" details the data and observations gathered from three primary studies conducted: 1) Recoil 2) Spinal Twisting and 3) Qualitative Observations.

1. Recoil: Sizing complications have been marked as one of the largest factors of LDR incompatibility. To mitigate this problem, Kresling origami is flat-fold and would theoretically be able to "recoil" to the appropriately-needed height between a patient's spinal discs; thus, a high recoil percentage is ideal for our origami LDR. Figure 11 demonstrates the discovered quadratic relationship between the number of kresling folds and recoil percentage.
2. Spinal Twisting: The twisting of spinal discs and LDRs is critical to ensure patients do not suffer from a loss of mobility and are able to regain their range-of-motion. Luckily, the LDR structure we proposed differs from currently-marketed LDRs because the top will be open for an increased range of motion. When evaluating the data, a higher spinal disc twisting capability is ideal to alleviate the current problem of limited mobility.
3. Qualitative Observations: From a birds-eye view (Figure 13), the four-fold structure mimicked a misshaped square rather than a traditional circle; thus, the benefits from the Kresling origami structure were not reaped, as evidenced by the low average recoil percentage and minimal twisting. The five-fold structure, though more closely resembling a cylinder, was much larger (Table 3) due to the pentagon structure. As a result, the circumference of the structure was much larger than the ideal size of a LDR. The seven-fold structure was similar to the six-fold structure but was firmer due to the excess folds and consequential smaller length. This firmness made the twisting of the prototype more difficult, as shown by the lower spinal twisting average angle measurement (Table 2). The eight-fold structure retained an oval-like shape, which is unlike a human's spinal disc.

From the recoil percentage study (Table 1), the six-fold structure retains the highest recoil capacity with an average percentage 90.9% with a standard deviation of ± 0.0059. When mimicking the twisting of a spinal disc, the six-fold structure also possessed the greatest movement with an average angle measurement of 19.8° with a standard deviation of ± 0.274 (Table 2). The data shown from both studies have a low standard deviation, demonstrating the data is statistically significant with a reasonably high degree of confidence. Thus, our selected number of Kresling folds was six for optimal recoil and capacity, while still accounting for qualitative observations from our prototypes.

Rough LDR Prototype

A rough prototype of the LDR was created for proof-of-concept. While the porous Titanium endplates were designed, modeled, and 3D printed as they are expected to be in the final prototype besides the keels, some aspects of the rough prototype do not match the design expectations for the final prototype given the limitations in materials and software available. The origami insert for the rough LDR prototype was made out of polyester sheets rather than elastomeric polyurethane. Nonetheless, the rough prototype was able to give a general idea of the functionality of the LDR design.

Rough Prototype Comparison

Three main comparison points were observed: 1) Recoil 2) Spinal Twisting and 3) Qualitative Observations. Data for the ActivL disc was acquired from the FDA data.

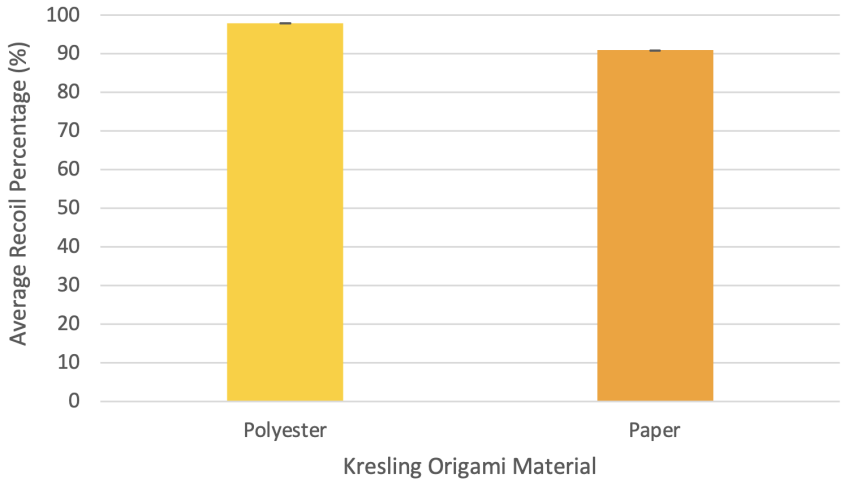

Figure 19. Average origami recoil percentage comparison between polyester (used in the rough prototype) and paper (used in the original design testing.)

1. Recoil: The polyester origami structure maintained an average recoil percentage of 98.4% with standard deviation of ± 0.0116, while the paper origami structure had an average recoil of 90.9% with a standard deviation of ± 0.0059 (Figure 19). As observed in Graph 2, the strength of the polyester is greater than the paper and allows for a larger recoil percentage.
2. Spinal Twisting: The polyester origami structure possessed a small maximum angle from twisting with 1.9° and a standard deviation of ± 0.268. The paper origami structure had a maximum twisting angle of 19.8° with a standard deviation of ± 0.274 (Table 2). Though the paper structure had a significantly higher average angle, mimicking a larger range of motion for the spine to twist, future steps will alleviate this issue as later addressed. As aforementioned, ActivL's primary complications stem from a lack of retained mobility after LDR surgery with range of mobility success only reaching 50%.
3. Qualitative Observations: The polyester structure maintains a much stronger structure in comparison to the paper prototype. This additional strength would serve to better survive in an anatomical environment, while still being biocompatible. The polyester is thicker than the paper, which accounts for the lower spinal twisting maximum angle, but the observed strength and recoil capacity of the material proved polyester to be the best material for our final implant.

Potential Risks

A potential risk was noted when observing the implant prototype made of polyester. While the free end of the insert was able to lock under the top endplate under small shear forces, it would slightly become dislocated under larger shear forces. A large concern for surgically-implemented biomedical devices is the potential for wear debris from the device becoming a danger once released into the body. For the proposed design, concerns were raised over the possibility of wear debris being released as a result of endplate-insert articulation. Future design modifications as later described have to be made in order to ensure that the articulation between the free end of the insert and the endplate is smooth and does not release debris.

Conclusion and Future Steps

In designing the LDR and assembling the rough prototype, many factors were taken into account. The load-bearing and motion requirements of healthy lumbar discs were considered, as well as how our prototype could be safely integrated into the body while retaining natural movement. Porous Ti-6AL-4V endplates were designed and 3D printed so as to best match the properties of natural lumbar discs. The optimal Kresling origami structure that would allow for maximum recoil and flexibility was identified after testing many different versions. Additionally, a method was proposed for synthesizing a chitosan sponge composite within the titanium endplates that can be loaded with antibiotics or growth factors to promote osseointegration and prevent infection.

Our current progress highlights the potential for a new origami-inspired LDR to mitigate complications such as incorrect sizing and poor osseointegration that are associated with currently-marketed LDRs. Our design, with its bioactive endplates and customizable fit, would be especially useful in improving the success rate of LDRs in patients suffering from other health concerns, like diabetes.

Future steps to assemble the final prototype are outlined in the Proposed Materials and Methods section. We hope to continue working on modifications that can mitigate the complications presented in the Potential Risks section. To prevent the dislocation of the free end of the insert under larger shear forces, we plan on deepening of the groove on the underside of the top endplate to hold the insert firmly in place under the forces that a human spinal disc normally endures. Furthermore, an addition of a thin capsule around the origami structure to reduce sharp edges and trap debris will eliminate the risk of wear debris entering the body.

Limitations

The data gathered throughout this report to determine the optimal number of folds was from a rough prototype folded from standard printer paper sheet. Polyester, our proposed material for the origami insert, is naturally thicker and more durable than paper, which may slightly alter the disc replacement's ability to effectively exhibit various forms of spinal twisting. However, we predict the discrepancies between the paper and polyester differences would be minimal due to the small change in thickness; additionally, the slight material change will harness the same optimality at six folds. When creating future prototypes, more data will be gathered to account for the recoil and spinal twisting effectiveness of polyurethane for more sustainable anatomical integration.

Other limitations in gathering data stem from human error in creating the prototypes. All prototypes were hand folded, which may have opened potential for human error in folding. The ends of the folded origami pattern were connected using hot glue. While we best tried to standardize the amount of hot glue used for each prototype, slight variations of the glue used are expected. Prototypes with more glue may have expressed more difficulty in recoiling because it creates a heighted barrier between the origami insert and mock endplate.

Current technology is still being developed to successfully create an FDA-approved, final version of the proposed design. The thickness we suggest for successful integration into the body is 2.0mm. However, 2.0mm is too thin for the currently available 3D printing services in porous titanium.

Acknowledgments

We would like to thank the MIT THINK Team, our mentors Mulan Jiang and Zimi Zhang, Professor Myron Spector (Massachusetts Institute of Technology), Professor Giovanni Traverso (Massachusetts Institute of Technology), Professor Hanqing Jiang (Westlake University), and the MIT THINK community for all of their guidance and support over the course of our project.

References

(PDF) theoretical pressure and friction in total disc ... (n.d.). Retrieved January 2, 2022, from https://www.researchgate.net/publication/279177241_Theoretical_pressure_and_friction_in_total_disc_prosthesis_f
or_lumbar_spine_Influence_of_ball_radius_and_biomaterial_combination

Biomedical implant devices fabricated from low Young's modulus titanium alloys demonstrating high mechanical
biocompatibility. (n.d.). Retrieved January 2, 2022, from https://www.sigmaaldrich.com/US/en/technical-documents/technical-article/materials-science-and-engineering/tissu
e-engineering/biomedical-implant-devices

Brinjikji, W., Luetmer, P. H., Comstock, B., Bresnahan, B. W., Chen, L. E., Deyo, R. A., Halabi, S., Turner, J. A.,
Avins, A. L., James, K., Wald, J. T., Kallmes, D. F., & Jarvik, J. G. (2015, April 1). *Systematic literature review of*
imaging features of spinal degeneration in asymptomatic populations. American Journal of Neuroradiology. Retrieved January 2, 2022, from http://www.ajnr.org/content/36/4/811

Cui, X.-D., Li, H.-T., Zhang, W., Zhang, L.-L., Luo, Z.-P., & Yang, H.-L. (2018, December 26). *Mid- to long-term*
results of total disc replacement for Lumbar Degenerative Disc Disease: A systematic review - Journal of Orthopaedic Surgery and research. BioMed Central. Retrieved January 2, 2022, from https://josr-online.biomedcentral.com/articles/10.1186/s13018-018-1032-6

DeJesus, Jenny. "What's the Link between Diabetes, Osteoporosis and Bone Fractures?" *HSS Playbook Blog*, 19
Feb. 2020, https://www.hss.edu/playbook/whats-the-link-between-diabetes-osteoporosis-and-bone-fractures/#:~:text=People%2
0with%20diabetes%20tend%20to,and%20strength%20of%20the%20bone.

Editors, M. (2016, March 10). Medgadget. Retrieved January 2, 2022, from https://www.medgadget.com/2016/03/origami-used-to-miniaturize-improve-surgical-tools-medical-implants.html

Fu, C., Yang, X., Tan, S., & Song, L. (2017, October 2). *Enhancing cell proliferation and osteogenic differentiation*
of MC3T3-E1 pre-osteoblasts by BMP-2 delivery in graphene oxide-incorporated PLGA/ha biodegradable microcarriers. Nature News. Retrieved January 2, 2022, from https://www.nature.com/articles/s41598-017-12935-x#Sec2

Guo, M., & Li, X. (2016). Development of porous Ti6Al4V/chitosan sponge composite scaffold for orthopedic
applications. Materials Science and Engineering: C, 58, 1177–1181. https://doi.org/10.1016/j.msec.2015.09.061

Hillson, Rowan. “The Spine in Diabetes - Wiley.” *Wiley Clinical Healthcare Hub*, 8 Feb. 2018, https://wchh.onlinelibrary.wiley.com/doi/pdf/10.1002/pdi.2149.

Kidambi, N., & Wang, K. W. (2020, June 5). *Dynamics of Kresling origami deployment*. Physical Review E. Retrieved January 2, 2022, from https://journals.aps.org/pre/abstract/10.1103/PhysRevE.101.063003

Lumbar Disk Replacement. Johns Hopkins Medicine. (n.d.). Retrieved January 2, 2022, from https://www.hopkinsmedicine.org/health/treatment-tests-and-therapies/lumbar-disk-replacement

Lumbar total disc replacement vs fusion: Which to choose. (n.d.). Retrieved January 2, 2022, from https://www.spineuniverse.com/treatments/surgery/lumbar-total-disc-replacement-vs-fusion

Medical Advisory Secretariat (2006). Artificial discs for lumbar and cervical degenerative disc disease - update: an
evidence-based analysis. *Ontario health technology assessment series*, *6*(10), 1–98.

Niinomi, M., Nakai, M., & Hieda, J. (2012). Development of new metallic alloys for biomedical applications. *Acta*
Biomaterialia, *8*(11), 3888–3903. https://doi.org/10.1016/j.actbio.2012.06.037

Oh, I.-H., Nomura, N., & Hanada, S. (2005, September 6). Microstructures and mechanical properties of porous
titanium compacts prepared by Powder Sintering. MATERIALS TRANSACTIONS. Retrieved January 2, 2022,
from https://www.jstage.jst.go.jp/article/matertrans/43/3/43_3_443/_article

Okpe, O. (2021, October 28). *Intervertebral discs*. Kenhub. Retrieved January 2, 2022, from https://www.kenhub.com/en/library/anatomy/the-intervertebral-discs

Pawar V, Bulbake U, Khan W, Srivastava R. Chitosan sponges as a sustained release carrier system for the prophylaxis of orthopedic implant-associated infections. Int J Biol Macromol. 2019 Aug 1;134:100-112. doi: 10.1016/j.ijbiomac.2019.04.190. Epub 2019 May 2. PMID: 31055114.

Pettine, K., Ryu, R., & Techy, F. (2017). Why Lumbar Artificial Disk Replacements (LADRs) Fail. *Clinical spine*
surgery, *30*(6), E743–E747. https://doi.org/10.1097/BSD.0000000000000310

Polo-Corrales, L., Latorre-Esteves, M., & Ramirez-Vick, J. E. (2014, January). *Scaffold design for Bone Regeneration*. Journal of nanoscience and nanotechnology. Retrieved January 2, 2022, from https://www.ncbi.nlm.nih.gov/pmc/articles/PMC3997175/

Yue, J. J., Garcia, R., & Miller, L. E. (2016, May 10). The ACTIVL(®) artificial disc: A next-generation motion-preserving implant for chronic lumbar discogenic pain. Medical devices (Auckland, N.Z.). Retrieved January 2, 2022, from https://www.ncbi.nlm.nih.gov/pmc/articles/PMC4869850/